

Hall-effect and resistivity measurements in CdTe and ZnTe at high pressure: Electronic structure of impurities in the zinc-blende phase and the semimetallic or metallic character of the high-pressure phases

D. Errandonea,^{1,2} A. Segura,^{1,3} D. Martínez-García,^{1,3} and V. Muñoz-San Jose³

¹Malta Consolider Team, 46100 Burjassot (Valencia), Spain

²Fundación General de la Universidad de Valencia Edificio de Investigación, C/Dr. Moliner 50, 46100 Burjassot (Valencia), Spain

³Departamento de Física Aplicada, ICMUV, 46100 Burjassot (Valencia), Spain

(Received 5 December 2008; revised manuscript received 30 January 2009; published 23 March 2009)

We carried out high-pressure resistivity and Hall-effect measurements in single crystals of CdTe and ZnTe up to 12 GPa. Slight changes in transport parameters in the zinc-blende phase of CdTe are consistent with the shallow character of donor impurities. Drastic changes in all the transport parameters of CdTe were found around 4 GPa, i.e., close to the onset of the cinnabar to rocksalt transition. In particular, the carrier concentration increases by more than five orders of magnitude. Additionally, an abrupt decrease in the resistivity was detected around 10 GPa. These results are discussed in comparison with optical, thermoelectric, and x-ray diffraction experiments. The metallic character of the *Cmcm* phase of CdTe is confirmed and a semimetallic character is determined for the rocksalt phase. In zincblende ZnTe, the increase in the hole concentration by more than two orders of magnitude is proposed to be due to a deep-to-shallow transformation of the acceptor levels. Between 9 and 11 GPa, transport parameters are consistent with the semiconducting character of cinnabar ZnTe. A two-orders-of-magnitude decrease in the resistivity and a carrier-type inversion occur at 11 GPa, in agreement with the onset of the transition to the *Cmcm* phase of ZnTe. A metallic character for this phase is deduced.

DOI: [10.1103/PhysRevB.79.125203](https://doi.org/10.1103/PhysRevB.79.125203)

PACS number(s): 72.80.Ey, 62.50.-p

I. INTRODUCTION

Even if transport measurements have been widely used in high-pressure research and have been applied to semiconductor physics since the foundational period,^{1,2} after the appearance of the diamond-anvil cell (DAC), optical measurements have certainly been the technique of choice in high-pressure semiconductor physics. However, in the last decade high-pressure transport experiments have shown to be a powerful tool to investigate pressure-driven changes in the electronic structure of semiconductors.³⁻⁵ Cadmium telluride (CdTe) and zinc telluride (ZnTe) are well-known II-VI semiconductors with a wide spectrum of technological applications; e.g., solar cells and α - and γ -ray detectors.⁶ Both tellurides upon compression undergoes a series of structural phase transitions which have been well documented in the literature.⁷⁻¹⁰ Despite the growing interest in the physical properties of CdTe and ZnTe, very little information currently exists on how their electrical properties are affected by compression. Two-points resistivity measurements have been done in CdTe by Samara¹¹ and Minomura.¹² Four-point resistivity measurements have been also performed but only in powder samples of CdTe using a DAC.¹³ In the case of ZnTe, only two-points resistivity measurements have been carried out.^{14,15} All these studies suffer from the drawback of being strongly affected either by contact resistance problems or carrier scattering at grain boundaries on powder samples. Additionally, in some cases, contradictory results have been published.^{11,13} More important, fundamental transport parameters such as the carrier concentration and mobility can only be obtained upon the performance of Hall-effect studies. In addition, important issues such as the semiconducting or metallic character of the high-pressure phases remains still

open. As a consequence of these facts, in order to provide accurate information of the pressure effects on the transport properties of CdTe and ZnTe we have performed resistivity and Hall-effect measurements in single-crystalline samples upon compression using a four-point technique. The experiments were performed in a quasihydrostatic setup up to 12 GPa. In Sec. II we will describe the experimental methods and the obtained results will be reported and discussed in Sec. III.

II. EXPERIMENTAL DETAILS

Single crystals here used were grown by the Bridgman method (CdTe) (Ref. 16) and the cold traveling heater method (ZnTe).¹⁷ Samples for transport measurements were cut from ingots with a wire saw, ground with abrasive powder, polished with diamond paste, and finally chemically polished with a 5% Br: methanol solution and washed in distilled water. CdTe crystals were *n*-type with typical resistivity 1.5 Ω cm, electron concentration 7.6×10^{15} cm⁻³, and mobility 550 cm²/V s at room temperature (RT). ZnTe crystals were *p*-type with typical resistivity 2.9×10^4 Ω cm, hole concentration 1.7×10^{13} cm⁻³, and mobility 12 cm²/V s at room temperature.

Hall-effect and resistivity measurements under pressure up to 12 GPa were made with steel-belted Bridgman tungsten carbide (WC) anvils with a tip of 15 mm in diameter. The samples were contained using two annealed pyrophyllite gaskets (0.5-mm thick each) in a split gasket geometry. The internal diameter of the gaskets was 5 mm and hexagonal boron nitride (BN) was used as pressure-transmitting medium. In our device, a 150 ton oil press is employed to apply

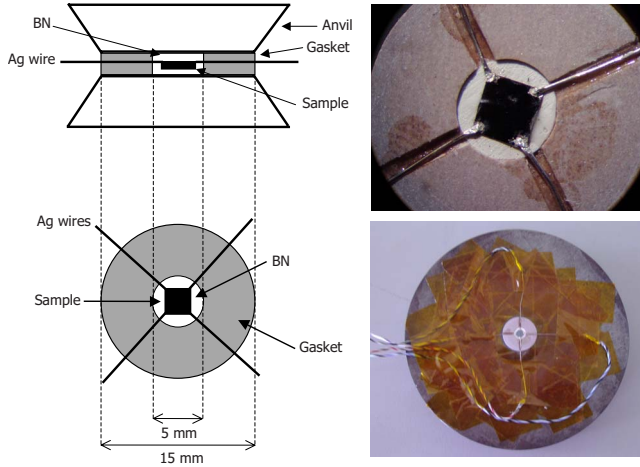


FIG. 1. (Color online) Schematic view of the opposed-anvils setup used in the transport measurements. A picture of a sample loaded in a pyrophyllite gasket, with contacts made on the Van der Pauw configuration, is shown together with a sample and pyrophyllite gasket mounted in a steel-belted WC anvil.

the load in two opposing WC anvils. Samples were typically 200- μm thick and $3 \times 3 \text{ mm}^2$ in size (sample 1). The pressure applied to the sample was determined by the calibration of the load applied to the anvils against high-pressure resistivity transitions in calibrants.¹⁸ The maximum pressure achieved with this setup is 13 GPa.¹⁹ Experiments were repeated two times for each material to check their reproducibility. A schematic view on the experimental setup and a picture of a loaded sample are shown in Fig. 1. Additional details of this setup can be found in Ref. 18. In CdTe, additional measurements constrained to 4 GPa were performed using larger WC anvils (27-mm diameter tip). In this case, the sample size was $5 \times 5 \text{ mm}^2$ (sample 2) and the pressure medium was sodium chloride. More details about this second high-pressure device can be found in Ref. 4. In CdTe the experiments were performed for pressure increase and release. In ZnTe we only report results for pressure increase since in the two experiments performed on it we suffered a contact breakage at 12 GPa.

In order to perform the transport measurements, four indium contacts were vacuum evaporated on the corners of the samples in the van der Pauw configuration, taking care that the contact size was always much smaller than the distance between the contacts (see Fig. 1). Silver (Ag) wires of 100 μm in diameter were used as electrical leads. To guarantee the good quality of contacts, the silver wires were flattened and sharpened at the tip, being soldered with high-purity indium to the evaporated indium electrodes. To avoid inaccuracy problems in the determination of the Hall coefficient (R_H) coming from offset voltages, we acquired two sets of Hall measurements: one for positive and one for negative magnetic field (0.6 T) directions. The linearity of the Ohmic voltages on the injected current was checked out at different pressures. From the performed experiments we obtained the pressure evolution of the resistivity (ρ), the electron (n) or hole (p) concentration, and the carrier mobility (μ).

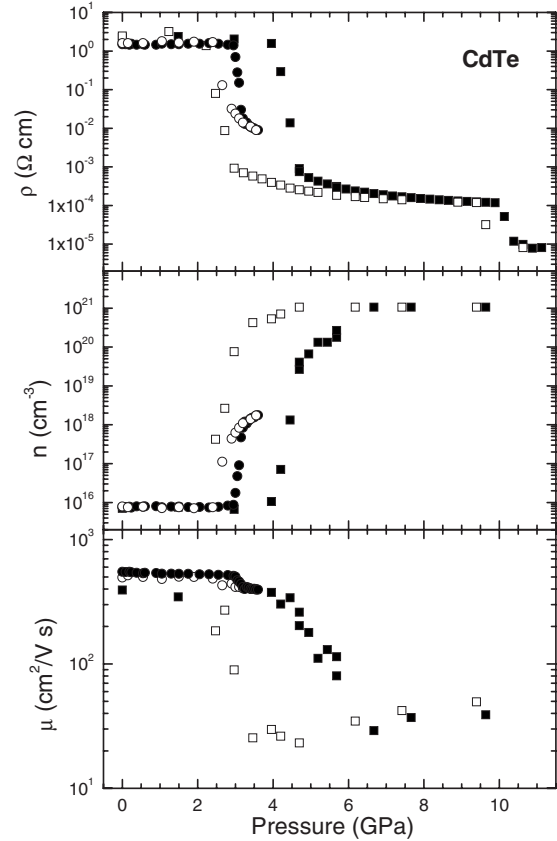


FIG. 2. Resistivity, carrier concentration, and mobility of CdTe at room temperature as a function of pressure. Solid symbols: up-stroke; Empty symbols: downstroke; Squares: sample 1; Circles: sample 2.

III. RESULTS AND DISCUSSION

A. Cadmium telluride

Figure 2 shows the pressure dependence of ρ , n , and μ in a CdTe sample as obtained from our measurements up to 12 GPa (sample 1). Up to 3 GPa, the only noticeable change is a slight decrease in the electron mobility that, given the constancy of the electron concentration, results in a slight increase in the resistivity. The decrease in the electron mobility is likely to be mainly determined by the increase in the electron effective mass, correlated with the increase in the band gap, according to the $\mathbf{k} \cdot \mathbf{p}$ model.²⁰ The pressure insensitivity of the electron concentration is consistent with the extrinsic conduction regime. All donor impurities are ionized at RT and the expected slight increase in their ionization energy under pressure does not change the donor level occupation probability.

The transition to the rocksalt phase⁷ is observed as abrupt changes in ρ , n , and μ at about 4 GPa, in agreement with x-ray diffraction experiments.^{7,8} Similar changes were observed in the experiments performed with the large anvils (sample 2), but in this case the onset of the changes took place at 3 GPa as can be seen in Fig. 2. This difference can be due, on the one hand, to the larger anvil surface that allows for a more progressive change in the pressure and a more detailed exploration of the pressure range through

which zinc-blende and cinnabar phases coexist. It is remarkable that changes in the transport parameters in this pressure range are fully reversible. On the other hand the much poorer quasi-hydrostatic conditions of the second set of experiments can also play a role. This observation is consistent with the fact that the zinc-blende–cinnabar–rocksalt structural sequence is sluggish,^{7,8,21} being affected by the experimental conditions. Indeed, it is a well-known fact that changes in the pressure-transmitting medium can reduce by several GPa the onset of a given phase transition.^{22,23} It is worth noticing here that, at a smaller scale, in sample 1 the onset of the transition is announced by a progressive increase in the carrier concentration above 3 GPa. Subsequently, after the abrupt changes observed between 4 and 4.5 GPa, a much slower increase is observed in n up to 6 GPa. On the other hand, the mobility decreases from 4 to 6 GPa, reaching a value of $3 \text{ cm}^2/\text{V s}$. However, the increase in the carrier concentration is the dominant effect producing the decrease in ρ reported in Fig. 2. Beyond 6 GPa the three transport parameters, ρ , n , and μ , remain nearly constant up to 10 GPa. Above this pressure, the Hall effect could not be measured because the Hall voltage became very weak. Nevertheless, an additional decrease in the resistivity, of more than one order of magnitude, could be detected in CdTe at 10 GPa, in agreement with the occurrence of the rocksalt to $Cmcm$ phase transition detected in x-ray diffraction experiments.⁷ All the changes found in the transport parameters are reversible. However a large hysteresis is observed for the changes induced at 4 GPa. This is not strange since on pressure release the zinc-blende phase of CdTe is only recovered at 2 GPa according with x-ray diffraction experiments.⁸ It is important to note here that from the decrease in ρ found at 10 GPa, an electron concentration of the order of $5 \times 10^{22} \text{ cm}^{-3}$ is estimated for the $Cmcm$ phase of CdTe, confirming that in this phase CdTe has a metallic character. This result is consistent with low thermoelectric power values ($S < 30 \text{ } \mu\text{V}/\text{K}$) measured above 10 GPa for the $Cmcm$ phase.²⁴

We would like to compare now our results with previous electrical measurements. Samara *et al.*¹⁰ and Shchennikov *et al.*,²⁴ using a two-point technique and single crystals of CdTe, observed a qualitatively similar pressure behavior for ρ than us, finding two sharp changes in the resistivity at 3.8 and 10 GPa. However, He *et al.*¹³ from their powder-sample experiments, reported a quite different evolution of ρ upon compression. These authors measured a continuous decrease in ρ with pressure, with three small inflexions at 4, 6.5, and 10 GPa. We think that the resistivity decrease reported by these authors below 4 GPa is an experimental artifact which can be quite possible related to contact problems in their powder samples, which is confirmed by the fact that they do not see any abrupt change in ρ at the rocksalt to $Cmcm$ transition (10 GPa). Indeed, the additional changes these authors reported for the resistivity at 15, 22.2, and 30 GPa (Ref. 13) are smaller than the scattering of their data and similar to the experimental uncertainties. Therefore their attribution to electronic transitions is not experimentally supported.

In order to provide a deeper interpretation of our results we will compare them with optical-absorption measurements.^{25,26} In these experiments, the transition to the rocksalt phase is observed at 3.8 GPa as a drastic decrease in

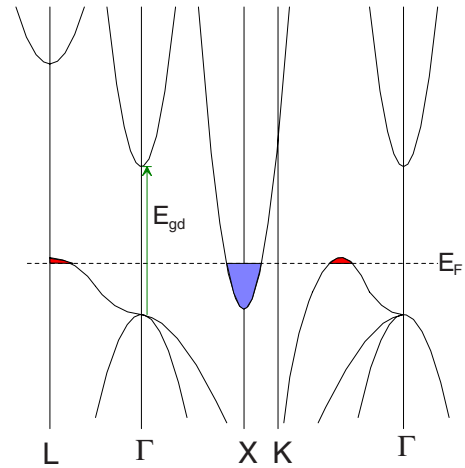


FIG. 3. (Color online) Proposed band structure of semimetallic rocksalt CdTe.

the sample transmittance. In particular, it was found that the sample becomes virtually opaque between 3.9 and 4.5 GPa. At this pressure, a range of relative transparency is observed between 1.2 and 2.2 eV. As pressure increases up to 10 GPa, the sample transmittance increases in the whole transparency range and the overall transmitted intensity increases by more than one order of magnitude. Different behaviors were observed in the low- and high-energy tails of the transparency range. While the low-energy tail tends to saturate and remains virtually constant above 6 GPa, the high-energy edge moves monotonously to higher photon energies as pressure increases.²⁵ Above 10 GPa the transparency region gradually shrinks and disappears at about 11 GPa.²⁵ These results were explained on the basis of the density-functional theory (DFT) band-structure calculations performed by Güder *et al.*²⁵ assuming that rocksalt CdTe is an indirect semiconductor with a small band gap. DFT calculations predict also a similar behavior for rocksalt ZnS and ZnSe.^{27,28} However, on the basis of our Hall-effect measurements and previous reflectance studies,²⁵ the low-gap model would be confirmed only under the assumption that the electrons filling the conduction-band minimum states in rocksalt CdTe are generated by extrinsic donor defects created at the phase transition. Given the constancy of the electron concentration above 6 GPa (around $1 \times 10^{21} \text{ cm}^{-3}$), as measured in two different samples, as well as the reversibility of the electron concentration on decompression, it seems more reasonable to assume that the free carriers have an intrinsic origin. This assumption necessarily leads to a semimetallic character for the rocksalt phase of CdTe. Such high-electron concentrations would not be observed in an intrinsic semiconductor at room temperature, even with a band-gap energy as low as a few tens of meV. Figure 3 shows a sketch of the proposed band structure of rocksalt CdTe around the Fermi level, based on the band-structure calculations reported in Ref. 25. Given the symmetry of the different points of the face-centered-cubic Brillouin zone, the conduction band consists of three equivalent valleys at the point X, while the valence band consists of four equivalent valleys at point L and twelve additional

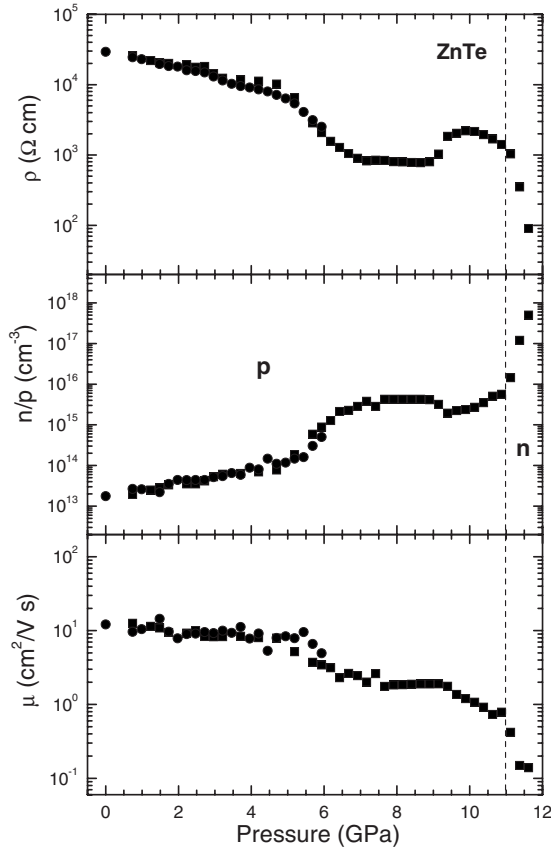


FIG. 4. Resistivity, carrier concentration, and mobility of ZnTe at room temperature as a function of pressure. Different symbols correspond to different samples. The vertical dashed line indicates the carrier-type inversion.

valleys in the GK direction. The density of states in the valence band is expected to be much larger than the one in the conduction band. This is the reason why the Fermi level is assumed to be at a larger energy from the bottom of the conduction-band minimum in the band sketch of Fig. 3.

The previous discussion also rules out the nonlinear behavior deduced for the band gap (E_g) of rocksalt CdTe from the pressure dependence of ρ in Ref. 13 assuming $\rho \propto e^{E_g/2kT}$, where k is the Boltzmann constant and T is the temperature. Such a direct correlation between resistivity and E_g can be expected only in an intrinsic semiconductor. In zincblende CdTe ($E_g \sim 1.4$ eV) the intrinsic carrier concentration is so low at RT that intrinsic samples would be virtually insulating. Free electrons are of extrinsic origin. Besides that, intergrain barriers in pellet samples preclude any attempt of relating resistivity changes to intrinsic parameters.

B. Zinc telluride

Figure 4 shows the pressure dependence of ρ , p , and μ in ZnTe sample as obtained from our measurements up to 12 GPa. There it can be seen that up to 5 GPa ρ smoothly decreases with pressure, mainly due to the increase in the hole concentration that compensates the slight monotonous

decrease in the hole mobility. From 5 to 7 GPa a one-order-of-magnitude decrease in the resistivity is observed due again to an increase in the hole concentration by two orders of magnitude, partially compensated by a decrease in the hole mobility by a factor 10. From 7 to 9 GPa both the hole concentration and mobility remain constant. At 9 GPa a rise of ρ starts, corresponding to a decrease in both the concentration and mobility, reaching the resistivity a maximum around 10 GPa. Beyond 11 GPa resistivity undergoes a very sharp decrease, associated to a carrier-type inversion and a quick increase in the electron concentration. These results are qualitatively in agreement with those reported by Ohtani *et al.*¹⁴ and Ovsyannikov *et al.*¹⁵ The carrier-type inversion was not detected in previous studies because the resistivity is insensitive to the sign change in the dominant charge carrier.

The values of the transport parameters at ambient pressure reveal the compensated character of these samples, consistently with photoluminescence (PL) measurements,²⁹ in which PL peaks between 540 and 600 nm were attributed to a large concentration of donor-acceptor pairs. The value of the hole mobility (about 12 $\text{cm}^2/\text{V s}$) is much lower than the intrinsic one (about 60 $\text{cm}^2/\text{V s}$),³⁰ which indicates ionized impurity concentrations between 1×10^{18} and 1×10^{19} cm^{-3} . As the hole concentration is about 2×10^{13} cm^{-3} , the ionized donor and acceptor concentrations must be of the same order $N_A \approx N_D \approx 5 \times 10^{18}$ cm^{-3} . In p -type compensated semiconductors, from the charge neutrality equation, it can be deduced that the hole concentration is given by the following expression:

$$p = \frac{N_V(N_A - N_D)}{2N_D} e^{-\Delta E_A/kT} \quad (1)$$

where N_V is the effective density of states in the valence band and ΔE_A is the acceptor ionization energy. PL results indicate the presence of acceptor levels with ionization energies up to 200 meV.²⁹

Let us discuss how changes in the transport properties induced by pressure can be correlated with changes in the electronic structure.

(i) As discussed above, the hole mobility is determined by ionized impurity scattering, and its decrease under pressure can be qualitatively explained. According to the $\mathbf{k} \cdot \mathbf{p}$ model²⁰ the effective masses of both heavy and light holes increase as the band gap increases.^{31–33} Also, the static dielectric constant of ZnTe decreases under pressure.³³ For ionized impurity scattering, both effects contribute to the decrease in the hole mobility under pressure.

(ii) The ionization energy of shallow acceptors increases under pressure due to the increase in the light hole effective mass and the decrease in the static dielectric constant.³³ This would necessarily lead to a decrease in the hole concentration under pressure, opposite to what is actually observed. Consequently, free holes must be generated by the ionization of deep acceptors, and the increase in the hole concentration must be associated to a decrease in their ionization energy under pressure. Between ambient pressure and 5 GPa the

hole concentration increases by a factor 10. Using Eq. (1), it is straightforward to determine the pressure coefficient of the acceptor ionization energy: $d\Delta E_A/dP = -11 \pm 2$ meV/GPa. This effect has been previously observed by other authors^{34–36} through PL measurements under high pressure. The deep character of ionized acceptors in Zn chalcogenides is attributed by these authors to a C_{3v} distortion of the substitutional acceptors^{34,35} or the Zn vacancy.³⁶ Under pressure the distortion decreases and eventually the distorted configuration becomes unstable with respect to the nondistorted configuration with local T_d symmetry. Remarkably, the pressure coefficient of the acceptor ionization energy, as measured through PL, is of the order of -10 meV/GPa, very close to the one obtained in this work from transport measurements.

(iii) At 6 GPa a further increase in the hole concentration is observed, leading to a constant value of 6×10^{15} cm⁻³ up to 9 GPa. In the framework of the distorted local configuration, 6 GPa would be the pressure at which the distorted configuration becomes unstable and the deep acceptor levels become shallow. Let us check the consistency of this model by applying Eq. (1) to estimate the concentration of ionized donors N_D . The constant hole concentration between 6 and 9 GPa can be assumed to be $p = N_A - N_D$. The ionization energy at 6 GPa would be the ionization energy of shallow acceptors, about 25 meV, as calculated from the light hole effective mass and static dielectric constant at this pressure.³³ From the total change in the hole concentration we estimate that ΔE_A decreases by 145 meV between ambient pressure and 6 GPa. Then the deep-level ionization energy at ambient pressure would be about 170 meV. If we calculate the effective density of states at the valence-band maximum from the heavy and light hole effective mass,³³ we get an estimation of $N_D \sim 8 \times 10^{18}$ cm⁻³, close to the one obtained above from the hole mobility at ambient pressure. Let us finally comment on the strong decrease in the hole mobility, associated to the acceptor deep-to-shallow transformation. As the total ionized impurity concentration does not change, the mobility decrease should be associated to an increase in the scattering cross section. This is what is expected in a deep-to-shallow transformation, in which the localized potential of a deep-level changes to a more extended Coulombian potential.

(iv) Regarding the change in the transport parameters observed around 9 GPa, it can be related with the occurrence of a pressure-induced phase transition to the cinnabar phase detected by x-ray diffraction measurements.^{9,14,15,37} Cinnabar ZnTe is a semiconductor with a band gap of some 1.2 eV.³⁸ The phase transition from zinc blende to cinnabar is a first-order one and the sample becomes polycrystalline. Carrier trapping and scattering at the grain frontiers explain the decrease in both the hole concentration and mobility, whose values around 10 GPa for ZnTe are close with those found for n and μ in the cinnabar phase of CdTe.

(v) Regarding the decrease in the resistivity and the increase in the carrier concentration observed beyond 11 GPa, these changes can be related with the presence of precursor defects of the transition to the $Cmcm$ phase of ZnTe.⁹ It is reasonable to assume that the introduction of the precursor defects leads to the creation of a large concentration of donor centers, which first compensate the acceptors of p -type ZnTe

and subsequently produce the observed carrier-type inversion, becoming the electron concentration

$$n = \frac{N_C(N_D - N_A)}{2N_A} e^{-\Delta E_D/kT}, \quad (2)$$

where N_C is the effective density of states in the conduction band and ΔE_D is the donor ionization energy. Note that this picture is also in agreement with the decrease in an order of magnitude found at 11 GPa in the carrier mobility. A value close to 0.2 cm²/V s is consistent with a highly defective crystal. A low mobility was also found beyond 9 GPa for the cinnabar of CdTe, indicating that this phase have a large concentration of defects too. It is worth commenting here that around 11 GPa a situation were both types of charge carriers, holes, and electrons contribute to transport properties could occur in a small pressure range. Under such situation the carrier concentration measured in Hall measurements (n_H) is

$$n_H = \frac{(p\mu_h + n\mu_e)^2}{p\mu_h^2 - n\mu_e^2}, \quad (3)$$

where μ_h and μ_e are the mobilities of holes and electrons. Therefore, a precise determination of the pressure where the type inversion takes place can be only made performing transport measurements at high pressure over a temperature range.

(vi) Finally, we would like to mention that the evolution of the electron concentration beyond 11 GPa suggests that as in CdTe, the $Cmcm$ phase of ZnTe has a metallic character. If the values we obtained for n from 11 to 12 GPa are extrapolated to 15 GPa, a pressure at which the cinnabar- $Cmcm$ transition is completed; a carrier concentration of around 1×10^{22} cm⁻³ is obtained. This value is in agreement with that estimated from optical reflectance measurements.³⁹ The conclusion on the metallic character of the $Cmcm$ phase is also in agreement with thermoelectric measurements previously performed in ZnTe.^{15,23} However, these studies were not conclusive regarding whether $Cmcm$ ZnTe has a metallic hole-like or electron-like conductivity. Our measurements support the second option.

IV. CONCLUSIONS

We reported high-pressure resistivity and Hall-effect measurements in n -type CdTe and p -type ZnTe up to 12 GPa. Continuous and reversible changes in the zinc-blende phase are consistent with the shallow character of donor levels in CdTe and a deep-to-shallow transformation of the acceptor levels in ZnTe. Concerning high-pressure phases, for CdTe, transport measurements have shown to be complementary with optical, thermoelectric, and x-ray measurements. In particular, the information provided by Hall-effect measurements has been crucial to decide between the low-gap semiconductor and semimetal models for rocksalt CdTe, in favor of the second option. In the case of ZnTe, the transition to the

cinnabar structure has been detected as abrupt changes in all the transport parameters. In addition, a carrier-type inversion and a sharp decrease in the resistivity were found at 11 GPa, being correlated with the onset of the transition to the *Cmcm* phase. For both CdTe and ZnTe it has been shown that the *Cmcm* phase has a metallic character with electron-like conductivity.

ACKNOWLEDGMENTS

This work was made possible through financial support of the MICINN of Spain under Grants No. CSD2007-00045, No. MAT2007-65990-C03-01, and No. MAT2007-66129 and by the Generalitat Valenciana under Grant No. GVPRE-2008-112.

- ¹P. W. Bridgmann, Proc. Am. Acad. Arts Sci. **56**, 61 (1921).
- ²P. W. Bridgmann, Proc. Am. Acad. Arts Sci. **72**, 157 (1938).
- ³D. Errandonea, A. Segura, J. F. Sanchez-Royo, V. Muñoz, P. Grima, A. Chevy, and C. Ulrich, Phys. Rev. B **55**, 16217 (1997).
- ⁴D. Errandonea, A. Segura, F. J. Manjon, and A. Chevy, Semicond. Sci. Technol. **18**, 241 (2003).
- ⁵D. Errandonea, A. Segura, F. J. Manjon, A. Chevy, E. Machado, G. Tobias, P. Ordejon, and E. Canadell, Phys. Rev. B **71**, 125206 (2005).
- ⁶*Properties of Wide Bandgap II-VI Semiconductors*, edited by B. Rameshwar, (Institution of Engineering and Technology, London, 1997); *Narrow Gap Cadmium Based Compounds*, edited by P. Capper (INSPEC, London, 1994).
- ⁷R. J. Nelmes, M. I. McMahon, N. G. Wright, and D. R. Allan, Phys. Rev. B **51**, 15723 (1995).
- ⁸D. Martinez-Garcia, Y. Le Godec, M. Mezouar, G. Syfosse, J. P. Itie, and J. M. Besson, Phys. Status Solidi B **211**, 461 (1999).
- ⁹R. J. Nelmes, M. I. McMahon, N. G. Wright, and D. R. Allan, Phys. Rev. Lett. **73**, 1805 (1994).
- ¹⁰A. Onodera, A. Ohtani, S. Tsuduki, and O. Shimomura, Solid State Commun. **145**, 374 (2008).
- ¹¹G. A. Samara and H. G. Drickamer, J. Phys. Chem. Solids **23**, 457 (1962).
- ¹²S. Minomura, G. A. Samara, and H. G. Drickamer, J. Appl. Phys. **33**, 3196 (1962).
- ¹³C. He, C. X. Gao, B. G. Liu, M. Li, X. W. Huang, A. M. Hao, C. L. Yu, D. M. Zhang, Y. Wang, H. W. Liu, Y. Z. Ma, and G. T. Zou, J. Phys.: Condens. Matter **19**, 425223 (2007).
- ¹⁴A. Ohtani, M. Motobayashi, and A. Onodera, Phys. Lett. **75A**, 435 (1980).
- ¹⁵S. V. Ovsyannikov and V. V. Shchennikov, Solid State Commun. **132**, 333 (2004).
- ¹⁶R. Triboulet, J. Alloys Compd. **371**, 67 (2004).
- ¹⁷R. Triboulet, K. P. Van, and G. Didier, J. Cryst. Growth **101**, 216 (1990).
- ¹⁸D. Errandonea, D. Martinez-Garcia, A. Segura, J. Ruiz-Fuertes, R. Lacombe-Perales, V. Fages, A. Chevy, L. Roa, and V. Muñoz, High Press. Res. **26**, 513 (2006).
- ¹⁹A. Segura, J. A. Sans, D. Errandonea, D. Martinez-García, and V. Fages, Appl. Phys. Lett. **88**, 011910 (2006).
- ²⁰E. O. Kane, in *The $k \cdot p$ Method, Semiconductors and Semimetals*, Vol. 1, edited by R. K. Willardson and A. C. Beer (Academic, New York, 1966).
- ²¹H. Sowa, J. Appl. Crystallogr. **38**, 537 (2005).
- ²²D. Errandonea, Y. Meng, M. Somayazulu, and D. Häusermann, Physica B **355**, 116 (2005); D. Errandonea, Y. Meng, D. Häusermann, and T. Uchida, J. Phys.: Condens. Matter **15**, 1277 (2003).
- ²³D. Errandonea and F. J. Manjon, Prog. Mater. Sci. **53**, 711 (2008).
- ²⁴V. V. Shchennikov and S. V. Ovsyannikov, Phys. Status Solidi B **244**, 437 (2007).
- ²⁵H. S. Güder, S. Gilliland, J. A. Sanz, A. Segura, J. Gonzalez, I. Mora, V. Muñoz, and A. Muñoz, Phys. Status Solidi B **235**, 509 (2003).
- ²⁶J. Gonzalez, F. V. Perez, E. Moya, and J. C. Chervin, J. Phys. Chem. Solids **56**, 335 (1995).
- ²⁷S. Ves, K. Strössner, N. Christensen, K. Kim, and M. Cardona, Solid State Commun. **56**, 479 (1985).
- ²⁸S. B. Qadri, E. F. Skelton, A. W. Webb, E. R. Carpenter, M. W. Schaefer, and J. Furdyna, Phys. Rev. B **35**, 6868 (1987).
- ²⁹J. A. Garcia, A. Remón, V. Muñoz, and R. Triboulet, J. Cryst. Growth **191**, 685 (1998).
- ³⁰T. Baron, K. Saminadayar, and N. Magnea, J. Appl. Phys. **83**, 1354 (1998).
- ³¹J. Wu, W. Walukiewicz, K. M. Yu, W. Shan, J. W. Ager, E. E. Haller, I. Miotkowski, A. K. Ramdas, and C. H. Su, Phys. Rev. B **68**, 033206 (2003).
- ³²A. Sotto, H. S. Güder, A. Pérez-Pastor, A. Segura, J. Zúñiga, and V. Muñoz, High Press. Res. **22**, 257 (2002).
- ³³M. Lindner, G. F. Schotz, P. Link, H. P. Wagner, W. Kuhn, and W. Gebhardt, J. Phys.: Condens. Matter **4**, 6401 (1992).
- ³⁴M. M. Li, D. J. Strachan, T. M. Ritter, M. Tamargo, and B. A. Weinstein, Phys. Rev. B **50**, 4385 (1994).
- ³⁵B. A. Weinstein, T. M. Ritter, D. Stracha, M. Li, H. Luo, M. Tamarg, and R. Park, Phys. Status Solidi B **198**, 167 (1996).
- ³⁶V. Iota and B. A. Weinstein, Phys. Rev. Lett. **81**, 4955 (1998).
- ³⁷A. San-Miguel, A. Polian, M. Gauthier, and J. P. Itié, Phys. Rev. B **48**, 8683 (1993).
- ³⁸A. Sotto, H. S. Güder, A. Pérez-Pastor, A. Segura, and V. Muñoz, High Press. Res. **22**, 315 (2002).
- ³⁹A. R. Goñi and K. Syassen, Semicond. Semimetals **54**, 247 (1998).